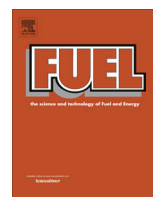




Contents lists available at ScienceDirect

Fuel

journal homepage: www.elsevier.com/locate/fuel

An experimental study of the reactivity of cellulosic-based chars from wastes



Lars Sørum^a, Paul A. Campbell^b, Nils Erland L. Haugen^{a,*}, Reginald E. Mitchell^c

^aSINTEF Energy Research, NO-7465 Trondheim, Norway

^bAgricultural and Biological Engineering, University of Technology, Jamaica

^cDepartment of Mechanical Engineering, Stanford University, USA

HIGHLIGHTS

- The reactivity of chars from wood chips, newspaper and glossy paper were studied.
- After devolatilization the chars had ash content in the range 2.2–61.8%.
- The reactivity of each of the chars were found to be a function of conversion.
- The by far most reactive char was the glossy paper, followed by the wood chip char.
- For reactivity measurements account must be made for the CO₂ ads. and des. of CaCO₃.

ARTICLE INFO

Article history:

Received 13 March 2013

Received in revised form 8 April 2014

Accepted 10 April 2014

Available online 30 April 2014

Keywords:

Cellulose
Combustion
Reactivity
Char

ABSTRACT

The objectives of this work were to determine the reactivity of the chars of different cellulosic-based wastes. In energy recovery from waste, the burnout of chars is a part of the overall complex combustion process. Being able to establish simple models for the char burnout process is therefore important. In this study, chars made from wood chips, newspaper and glossy paper were chosen as being representative of the cellulosic fractions of municipal solid waste. The ash content of these parent materials ranged from 0.4% to 24.8% by weight, on a dry basis. After devolatilization, the chars had ash contents in the range 2.2–61.8%.

The reactivities of the chars examined were determined from weight loss and surface area measurements. Weight loss was measured via thermogravimetry and surface areas were measured via gas adsorption techniques using CO₂ as the adsorbing gas.

The reactivity of each of the cellulosic-based chars was found to be a function of conversion. The glossy paper char was found to be much more reactive than the wood-chip char, which in turn was found to be slightly more reactive than the newspaper char. In order to obtain the reactivity for the glossy paper char from the gravimetric measurements, it was crucial to account for calcium carbonate in the sample, a clay used in the paper-making process to give the paper its glossy appearance. Calcium carbonate (CaCO₃) desorbs CO₂ at the high temperatures used during char preparation and adsorbs CO₂ at the low temperatures used in the reactivity tests to ensure kinetics-limited oxidation.

The average intrinsic reactivities for the three chars, during reaction in 10 vol.% oxygen at 500 °C and atmospheric pressure, were found to be 0.46×10^{-6} , 0.21×10^{-6} and 1.36×10^{-6} g m⁻² s⁻¹, respectively, for the wood-chip, newspaper and glossy-paper chars and the corresponding peak reactivities were 1.43×10^{-6} , 1.06×10^{-6} and 5.80×10^{-6} g m⁻² s⁻¹. The reactivities for the chars differ as a function of conversion and ash content, but no trend in terms of either increasing or decreasing reactivity with increasing ash content was found. Moderate heat treatment, where the char is exposed to 1277 °C for 47 ms, had no significant influence on char reactivity.

© 2014 Elsevier Ltd. All rights reserved.

* Corresponding author. Tel.: +47 98608683.

E-mail address: nils.e.haugen@sintef.no (N.E.L. Haugen).

Nomenclature

m	mass of char particle, kg	$W_{c,a}$	$= W_c + W_{CO_2}$, kg
m_0	initial mass of char particle, kg	W_c	mass of the carbonaceous part of the char, kg
R_c	specific mass loss rate of char, s^{-1}	$W_{c,0}$	initial mass of the carbonaceous part of the char, kg
R_{ic}	intrinsic chemical reactivity per unit mass specific surface area, $kg\ s^{-1}\ m^{-2}$	W_{CO_2}	mass of the CO_2 captured by the CaO, kg
\bar{R}_{ic}	average intrinsic chemical reactivity, $kg\ s^{-1}\ m^{-2}$	$W_{CO_2,M}$	total mass of the CO_2 which can be captured by all the CaO, kg
S_{ga}	specific surface area of the ash part of the char, m^2/kg	W_p	mass of char particle, kg
S_{gc}	specific surface area of the carbonaceous part of the char, m^2/kg	$W_{p,0}$	initial mass of char particle, kg
$S_{gc,0}$	initial specific surface area, m^2/kg	X_a	mass fraction of ash
S_{gp}	surface area per unit mass of char particle, m^2/kg	x_c	fractional char conversion
S_v	volume specific surface area, m^2/m^3	ψ	structural parameter
t	time, s	ρ_p	apparent mass density of char particle, kg/m^3
W_{ash}	mass of the CO_2 free ash, kg		

1. Introduction

The awareness of the environmental consequences connected to waste disposal together with the large amounts and inhomogeneous nature of municipal solid waste (MSW) has led to complex waste management systems. Material reuse/recycling, anaerobic digestion, composting and combustion with energy recovery are some of the methods that are used in addition to landfilling. The lack of landfill sites and assessments of the environmental consequences of landfilling have led many countries to ban landfilling of combustible wastes, including wet organic waste. This development has led to an increase in the amount of MSW that is subjected to energy recovery. The increasing utilization of MSW for energy recovery also increases the total amount of residues from energy from waste plants. This has led to an increasing interest in utilization of residues from the combustion process such as using fly ashes as a filling material in concrete and bottom ashes as road filling material. However, it is important to be aware of the fact that utilization of residues from MSW combustion sets requirements to ash quality. Knowledge on the burnout process of chars in MSW combustion is therefore important. In energy recovery from municipal solid waste, the burnout of chars is a part of the overall complex combustion process. Being able to establish simple models for the different phases of the combustion process such as drying [1], devolatilization [1,2], combustion of volatiles [3] and the subsequent char burnout is important. MSW consists of many different fractions such as paper/cardboard, plastics, glass, metals, wet organic wastes (e.g., yard and food wastes), and other combustible (e.g., wood and rubber) and non-combustible (e.g., sand and ashes) wastes. The major proportion of char from MSW originates from cellulosic wastes such as paper, cardboard, wood and other organic wastes. The composition may vary to a great extent in MSW. It is therefore important to establish information on the reactivity of the different cellulosic based chars during char burnout. This work is part of an ongoing effort to develop a physical model describing the burnout of chars. Being able to determine the reactivity of the different chemical structures of cellulosic materials will enable us to better understand, and therefore, model more accurately the burnout process.

2. Experimental approach**2.1. Materials selected for study**

The parent materials, wood chips (WC) and two different types of paper, newspaper (NP) and glossy paper (GP) were chosen to

represent the cellulosic portion of MSW. The proximate and ultimate analysis of the parent materials are shown in Table 1. Noted are the lower volatile matter and fixed carbon contents of the GP and its correspondingly higher ash content.

Analysis of the ashes of the three parent materials are given in Table 2. The results indicate that the major inorganic elements present in each of the three materials are calcium (measured as CaO), aluminum (measured as Al_2O_3) and silicon (measured as SiO_2). Many biomass materials have extraneous inorganic compounds composed of these elements, which were added to the carbonaceous substrate through geological processes as well as during harvesting, handling and processing. A significant fraction of the calcium reported for the GP is believed to be associated with the clays that were used in the paper-making process. Calcium carbonate ($CaCO_3$) and kaolin ($Al_2Si_2O_5(OH)_4$) are amongst the clays that are commonly used to give glossy paper its appearance. Based on the relatively low aluminum content and high calcium content of the ash, $CaCO_3$ is the clay most likely to have been used in making the glossy paper employed in this study. The exact amount of clay added to make the glossy paper used is unknown, however according to paper manufacturers, clays can consist of as much as 45%, by weight, of the mixture used to produce the glossy paper. The balance of the ash components represent the combined concentrations of the trace inorganic elements in biomass materials as well as unknown components in the clays and inks used to make and print the glossy paper. Our investigations indicate that the addition of 35% calcium carbonate and 3.7% kaolin yield C, H and O elemental weight fractions that agree with the measurements.

2.2. Char preparation

Chars for this study were prepared under different conditions. A tube furnace (TF) was used to prepare chars at a heating rate of $35\ ^\circ C/min$ in an inert environment. The chars prepared in the TF were devolatilized in a nitrogen environment at $900\ ^\circ C$. Chars prepared in the TF are denoted LH (low heating rate) in this paper. Some chars were first prepared in the TF at the low heating rate and then samples were injected into an entrained laminar flow reactor (LFR) in which a high-temperature (nominally $1277\ ^\circ C$), nearly inert (O_2 concentration in the parts-per-million range) environment was established. Particle heating rates in the LFR were of the order of $105\ ^\circ C/s$. Chars injected into the LFR are denoted HT (heat-treated) in this paper. Since the residence time in the LFR is only 47 ms, the mean temperature increase of the particle is relatively small.

The proximate and ultimate analysis of the LH-chars produced from the parent materials are shown in Table 3. Based on the ash contents of the parent materials and their chars, under the low heating-rate conditions of the tube furnace, volatile yields for the wood chips, newspaper, and glossy paper were 81.8%, 69.6%, and 59.9%, respectively. As observed, all the chars produced at the low heating rate contain volatile matter, the GP char having a significant amount. The GP char also has a relatively high content of oxygen and a corresponding lower content of carbon (on an ash-free basis) compared to the two other chars. It should be mentioned that the proximate and ultimate analysis were performed by a commercial company, following the standard ASTM procedures for making such analysis.

Since the oxygen content in an ultimate analysis is calculated by difference, what is reported as the oxygen content for the GP char is likely to be influenced by the CaCO_3 and other clays added to give the GP its glossy appearance. When the GP sample is heated to the high temperatures used in performing the ultimate analysis, CaCO_3 releases oxygen in the form of CO_2 , yielding calcium oxide (CaO) in the ash.

A schematic drawing of the LFR system used to heat-treat the chars, including the solids sampling probe positioned along the axis of the LFR, is shown in Fig. 1. The fuel (a mixture of methane and hydrogen) and the oxidizer (a mixture of oxygen and nitrogen) are led to the burner in separate supply lines. When ignited, the

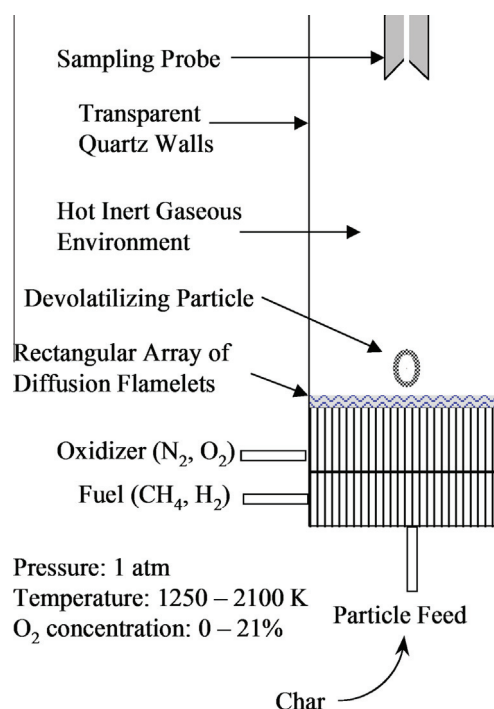


Fig. 1. Schematic drawing of the laminar flow reactor. The temperature in the reactor is 1277 °C, while the residence time of the particles are 47 ms.

Table 1

Proximate and ultimate analysis of parent materials. The oxygen fraction is obtained by difference to satisfy the mass balance. Volatile matter is determined following the ASTM D 3175-07 standard, where it is being heated to 950 °C. The chlorine content of the chars is expected to be very low since the cellulosic fractions are based on virgin wood. Furthermore, the clays used in the GP char does not contain any chlorine.

Parent material	Proximate analysis (dry)			Ultimate analysis (daf)				
	VM (wt%)	Fixed C (wt%)	Ash (wt%)	C (wt%)	H (wt%)	O (wt%)	N (wt%)	S (wt%)
WC	86.3	13.3	0.4	47.7	6.2	46.0	0.1	<0.02
NP	85.9	10.7	3.5	46.3	6.0	47.6	0.1	<0.02
GP	70.6	4.5	24.8	41.9	5.3	52.7	0.1	<0.02

Table 2

Ash analysis of the parent materials.

Component	WC	NP	GP
SiO_2	27.29	40.49	4.84
Al_2O_3	4.58	26.30	4.12
TiO_2	0.27	0.16	0.07
Fe_2O_3	5.83	0.64	0.17
CaO	33.00	21.40	54.10
MgO	7.39	1.98	0.65
Na_2O	2.17	0.96	0.55
K_2O	6.54	1.14	0.05
P_2O_5	3.46	0.29	0.05
SO_3	3.44	1.21	0.06
balance	6.03	5.43	35.34

Table 3

Proximate and ultimate analysis of LH-chars of the parent materials. The oxygen fraction is obtained by difference to satisfy the mass balance.

Char (wt%)	Proximate analysis			Ultimate analysis (daf)				
	VM (wt%)	Fixed C (wt%)	Ash (wt%)	C (wt%)	H (wt%)	O (wt%)	N (wt%)	S (wt%)
WC	7.6	90.2	2.2	98.58	0.4	0	1.0	0.02
NP	9.4	79.1	11.5	98.1	0.8	0	1.0	0.1
GP	21.4	16.8	61.8	73.6	1.7	23	1.1	0.6

fuel and oxidizer burn on the burner surface, creating an array of diffusion flamelets. The temperature and gas composition profiles established in the LFR are controlled by the compositions of the inlet fuel and oxidizer mixtures and their mass flow rates. Since in this study the LFR was used only to produce chars at a high heating rate, (and not to produce partially reacted chars for examination), inlet gas flow rates were adjusted to establish a nearly inert environment in the LFR, and the sampling probe was placed at a position just above the point where devolatilization ended for extracting particles. Specific details of the LFR and its isokinetic solids sampling probe have been presented in previous work [4].

All the solid materials used in this study were ground and wet-sieved to yield a distribution of particles having diameters between 106 and 125 μm . The particles were injected into the LFR at a rate between 0.3 and 0.5 g/hr, and solid samples were extracted at a residence time of 47 ms. The NP-LH char was injected into the LFR to yield a heat-treated char at 35% weight loss (denoted NP-HT). Based on 35% weight loss (estimated from the weight of material fed to the LFR and the weight of char collected), the ash content of the NP-HT is 17.7%.

The chars produced in this study are representative of the range of chars produced in a real grate furnace. In a grate furnace, the parent materials of the real chars (wet waste) enter the furnace and travel along the inclined grate where they undergo all the sub-processes that constitute the whole combustion process. In general, one can describe the process as follows: At the first section of the grate, the waste dries, then devolatilizes at the second section. The volatiles mix with the oxidizer coming from the bottom of the grate and burn on top of the grate and in the secondary combustion chamber. At the last section of the grate, the chars created during devolatilization burnout, and the remaining ash is transported to an ash container. The parent material can spend up to 2 h on the grate during this whole combustion process. Typically, the height of the waste bed on the grate is 30–50 cm. Depending on if the waste is directly exposed to the burning flame on top of the grate or if it is only heated up by surrounding particles and

hot gas, the chars produced from the parent materials may experience some heat treatment.

Visualizing the samples is useful in order to get a better understanding and knowledge on the materials properties. Ordinary digital pictures of the parent materials and scanning electron microscope (SEM) pictures of the different powdered parent materials and chars are shown in Table 4. Wood chips and newspaper in this study have similar chemical compositions. The reason for this similarity is that newspaper is made out of wood chips or wood by mechanical processing (i.e., only mechanical processing of wood produces mechanical pulp (fibers) for paper production; no chemicals are added). The only difference is the adding of color or ink in the newspaper production process. Glossy paper is also made of wood fibers, but the quality of the paper used might differ from newspaper. Glossy paper can consist of mixtures of mechanically-processed wood pulp and chemically- or partially chemically-processed wood pulp. As already mentioned, in the production process of glossy paper, kaolin and calcium carbonate are often used as filling material to obtain the proper glossy finish.

As can be observed from the SEMs, all chars have open structures with visible pores. Also shown in the SEMs of the glossy paper char is the large amount of ash present as the flat dense portions of the char.

In order to investigate the influence of ash on reactivity of cellulosic-based chars, several attempts to remove ash from the glossy paper char, the char containing the most ash, were made. Ash removal was made by acid washing GP-LH samples using hydrogen chloride in one case, and a solution of ammonium acetate in another. However, both attempts to remove ash by acid washing also altered the reactivity of the remaining char, as evidenced in our combustion tests. To obtain char samples with lower ash contents without altering the chemical reactivity of the material, chars were washed in hot water for 16 h at 80 °C, as described by Miles et al. [5]. The hot water washing resulted in a char (designated GP-WW) having an ash-content of 53%. Separate density fractions of the GP-LH char were also obtained via sedimentation in cold water. Density-separation in cold water yielded chars

having ash contents of 37% and 45%. These chars behaved similarly in combustion tests; only the 37% ash-content glossy paper char (referred to hereafter as GP-DS) is discussed. Insufficient char was available for surface area measurements of the GP-DS char. The specific surface area was assumed to be similar to that of GP-LH.

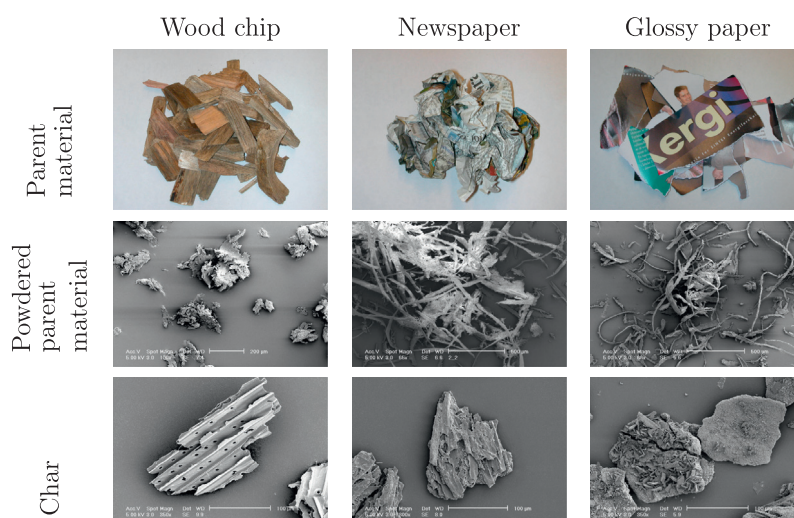
2.3. Combustion tests

Combustion tests used to determine the reactivity of char samples were performed in a pressurized thermogravimetric analyzer (PTGA), which was modified to yield information about the gas composition during the course of reaction. The experimental setup of the PTGA and control and data acquisition system is shown in Fig. 2.

The PTGA used in this study is a TG151 manufactured and delivered by Thermo Electron, and is designed for a temperature range of 20–1100 °C and pressures from 0.13×10^{-6} bar to 100 bar. The sensitivity is 10^{-6} g and the weight range is 0–100 g. An “empty pan” test is run before all reactivity tests in order to account for buoyancy and drag forces acting on the sample pan due to the upward flow of reactive gases past the sample pan. The “empty pan” measurements are subtracted from the measurements obtained with a measured quantity of sample in the pan in order to get mass measurements free of buoyancy and drag effects.

An optimal char sample size is employed so that the measured weight loss can be maximized while still maintaining negligible mass transfer effects on the measured reaction rate. Measured weight loss increases with sample size, but diffusional resistances through large sample sizes prevent accurate measurement of the true kinetic rates with large samples. In our procedure to determine an optimal sample size, successively smaller sample sizes were tested in the TGA until the measured char mass loss conversion profiles were no longer a function of sample size. In reactivity tests of the char of Illinois No. 6 coal, Tsai [6] found that samples sizes less than 0.12 g at 1 atm and less than 0.06 g at 25 atm yielded mass loss profiles that were essentially the same,

Table 4
Pictures of parent materials, powdered parent materials and chars.



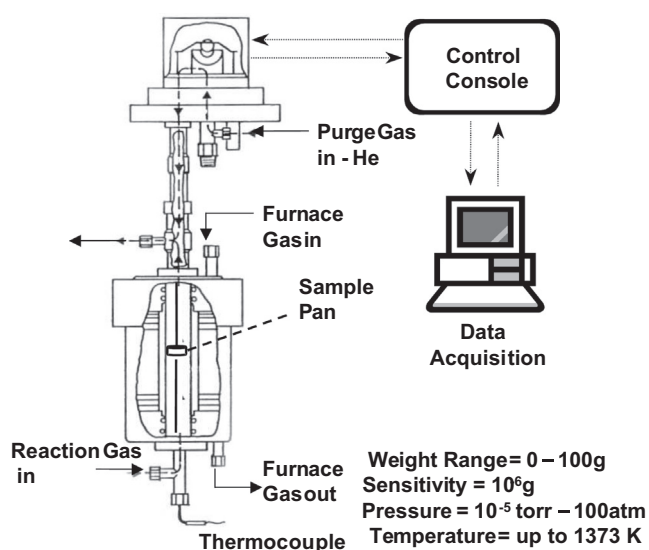


Fig. 2. Experimental set-up of the PTGA, control and data acquisition system.

indicative of mass transport-free measurements. In all reactivity tests reported in this work, an initial char sample weight of approximately 0.02 g (20 mg) was used.

The 1-cm diameter sample pan used had a mesh bottom in order to let the reaction gas, entering from below the sample, have unrestricted access to the sample. The reaction gas composition, reactor temperature and data acquisition are all controlled by a control unit during a combustion test. More detailed information on the specifics of the PTGA is also presented elsewhere [6].

Shown in Fig. 3 are experimental results from a typical combustion test in the PTGA performed at atmospheric pressure, at 500 °C and with an oxygen concentration of 10 vol-%, conditions in which the mass loss rates were controlled by the intrinsic reactivity of the carbonaceous material. After the sample has been put in the pan and the PTGA is closed, the reactor is purged with nitrogen for 53 min at room temperature to ensure an inert environment. Any CO₂, CO or air, remaining in the reactor chamber is eliminated during this time. After 53 min, the temperature is ramped up to the reaction temperature of 500 °C in 20 min, still in an oxygen-free environment in order to dry the sample. As can be observed from the flat portion of the weight profile from 75 to 90 min, the sample is dry before the reaction gas is admitted. During this heating and drying of the sample in nitrogen, a small amount of CO and CO₂ is

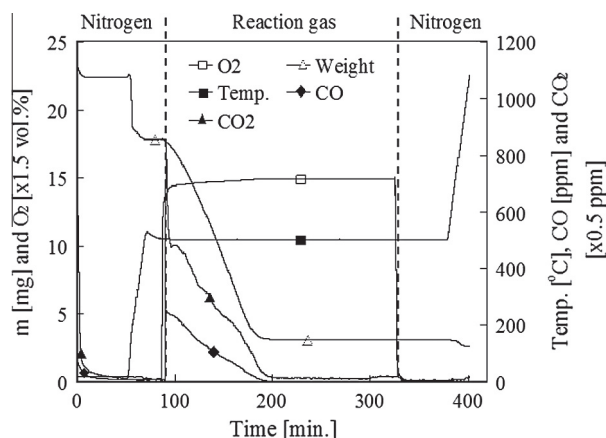


Fig. 3. Experimental results from a typical combustion test in 10 vol-% O₂ in the PTGA.

released (desorbed). These carbon oxides are formed from oxygen complexes in the initial char sample.

At 90 min, the reaction gas (10 vol-% O₂) is turned on. From 90 to 330 min (240 min reaction time) the particle is kept at a constant temperature (500 °C) and in a uniform and constant gas composition. During the reaction period, the oxygen reacts with the carbon in the sample, producing CO and CO₂, which are subsequently released, reducing the mass of the material on the PTGA balance pan. At 330 min the reaction gas is turned off and the sample is once again purged with nitrogen, making sure that the sample is no longer reacting. At 378 min, still in nitrogen, the sample is heated up till 1100 °C in order to remove any adsorbed oxygen complexes remaining on the material in the balance pan. This yields the true sample mass at the end of the test. The oxygen on the sample during this desorption is released as CO and CO₂ if there is still carbon left in the sample. With the GP, CO₂ is also released when the temperature is increased to 1100 °C at the end of the combustion tests as a result of CaCO₃ decomposition. Calcium carbonate is stable at temperatures below about 600 °C but dissociates, releasing CO₂ at higher temperatures.

In a parallel study to obtain the pyrolysis kinetics of these same parent materials, it was revealed that WC and NP had practically the exact same weight loss profiles as a function of temperature. This is another indication of the similarity of the chemical composition of these two materials. Weight loss profiles as a function of temperature or thermograms such as this are often used to fingerprint different types of materials.

2.4. Surface area measurements

The specific surface areas of the char particles used in the combustion tests were measured employing the BET procedure [7,8], using CO₂ as the adsorption gas [9]. The surface area measurements were done *in situ* during a combustion test in the PTGA, yielding the surface area per unit mass of particles, S_{gp} , as a function of char conversion. To obtain *in situ* measurements, the combustion tests were interrupted at selected extents of conversion by rapidly switching from the reactive gas to nitrogen and lowering the temperature to room temperature, performing the CO₂ adsorption measurements, and then reheating the partially oxidized sample back to the reaction temperature in nitrogen before readmitting the reactive gas to continue char oxidation. The CO₂ adsorption measurements were made at room temperature and 10 atm. Information about the specifics on the BET experiments can be found elsewhere [6,10].

3. Data analysis

The char particles are assumed to consist of two components: an ash fraction, which is assumed to be non-reactive below a certain temperature, and a carbonaceous fraction, which is assumed to react with oxygen, forming both CO and CO₂. The specific mass loss rate of the char (R_c) is expressed in terms of the mass loss rate and specific surface area of the carbonaceous portion of the particle material (S_{gc}) as:

$$R_c = -\frac{1}{W_c} \frac{dW_c}{dt} = \frac{1}{1-x_c} \frac{dx_c}{dt} = R_{ic} S_{gc} \quad (1)$$

where W_c is the mass of carbonaceous material in the char at time t ; x_c is the fractional char conversion on a dry and ash free (daf) basis; S_{gc} is the mass specific surface area of the carbonaceous material (in m²/kg); and R_{ic} is the intrinsic chemical reactivity per unit mass specific surface area.

During char oxidation, the volume-specific surface areas (S_v , in m²/m³) of particles change, increasing due to micro-pore reactions

and decreasing due to pores merging and coalescing. Early in burnoff the change in surface area is due primarily to the opening of initially closed-off pores, creating new interconnections that expose additional surface area. Owing to this competition between the exposure of new pore surface area and loss of pore surface area due to pores merging and coalescing, there is a maximum in the volume specific surface area with conversion. The mass specific surface area, which is related to the volume specific surface area through the particle's apparent density ($S_v = \rho_p S_{gc}$), progressively increases with char conversion until quite late in burnoff under kinetically-controlled conversion conditions.

The specific surface area of the ash-containing particle (S_{gp}) is measured, it is, however, the specific surface area of the carbonaceous portion of the char (S_{gc}) that is needed to extract the intrinsic reactivity from the weight loss measurements. To determine S_{gc} , the following expression is used:

$$S_{gp} = (1 - X_a)S_{gc} + X_a S_{ga}. \quad (2)$$

Here, S_{ga} is the specific surface area of the ash and X_a is the instantaneous mass fraction of the ash, calculable from the initial ash content of the char and the extent of conversion. Measurements made during this work and the work of Campbell et al. [10] suggest that the mass specific surface areas of ashes from both biomass and coal are in the range 5–10 m²/g, considerably lower than values determined for the mass specific surface areas of coal and biomass char particles. Hence, the mass specific surface area of the ash is inconsequential until late in burnoff.

An expression for R_{ic} was determined from Eq. (1) to yield:

$$R_{ic}(x_c) = \frac{R_c(x_c)}{S_{gc}(x_c)} = \frac{dx_c/dt}{(1 - x_c)S_{gc}(x_c)}. \quad (3)$$

Quantities on the right-hand-side of this equation are determined from the measurements, permitting the evaluation of R_{ic} as a function of conversion at the test temperature.

4. Results and discussion

4.1. Specific surface area and oxidation thermograms

Shown in Fig. 4 are the measured mass specific surface area evolution profiles for the different chars as a function of conversion. The initial mass specific surface areas of the chars are nearly the same, in the range 366–409 m²/g. This is largely due to the similarity in the chemical make-up of the cellulosic materials selected for study and the uniformity in the devolatilization conditions. All of the chars, with the possible exception of the glossy paper, exhibit a monotonic increase in mass specific surface area with conversion up to at least 60% conversion. The wood chip and newspaper

chars formed at the low heating-rate condition exhibit similar increases in specific surface area up to 80% conversion. There is only a modest difference in the surface area evolution of the NP-LH and NP-HT chars at low conversions. With increased conversion, the differences become more apparent, the heat-treated char showing the smaller increase in mass specific surface area with conversion.

The solid lines in Fig. 4 are calculations based on the random pore model for chemical-kinetics controlled conversion of porous materials developed by Bhatia and Perlmutter [11]. The model is used to predict the variations in the volume specific surface area with conversion. Since under kinetically controlled char conversion particle apparent density is proportional to particle mass loss, the following expression can be derived for the mass specific surface area variation with conversion from the Bhatia and Perlmutter model:

$$S_{gc} = S_{gc,0} \sqrt{1 - \psi \ln(1 - x_c)}. \quad (4)$$

In our approach, the initial mass specific surface area ($S_{gc,0}$) and the structural parameter ψ are found from a least squares fit to the experimental data. The solid lines shown in Fig. 4 are based on such list squares fits. Values determined for ψ are presented in Table 5.

The chars produced from glossy paper at the low heating rate condition, GP-LH and GP-WW, also exhibit an initial increase in mass specific surface area with increase in conversion. In the 25–35% conversion range, there appears to be a peak in the mass specific surface area of the GP-LH char, but such a peak is not consistent with the prediction of the random pore model. It is important to note that the surface area measurements of the GP chars are likely to be influenced by the amount of calcium in the ash, for any CaO in the ash can react with CO₂ to form CaCO₃. Consequently, the CO₂ uptake measured in the BET adsorption tests is not solely a consequence of CO₂ adsorption on carbonaceous surfaces but also depends on the concentration of CaO in the char. Uncertainties in the specific surface area measurements are expected to increase with conversion, as the char contains less and less carbonaceous material and more ash as conversion progresses.

At 50% conversion, the GP-LH char is comprised of about 77% ash, which has a lower mass specific surface area than the carbonaceous material. If the specific surface area of CaCO₃ is larger than 5 m²/g (the value assumed for the mass specific surface area of the biomass ash), the mass specific surface area values reported for the char would be too low. This could explain the observed decrease in the surface area of the GP-LH char for $x_c > 0.5$, when the char is comprised mostly of ash.

It is clear that there are relatively large uncertainties involved in the determination of the surface area of the GP chars, especially at high conversions. Based on the similarities in the initial mass specific surface areas of the NP and GP chars, it is reasonable to expect for the carbonaceous portions of the chars to evolve similarly, which seems to be the case for all the chars produced at the lower heating rate. In our approach to determine the intrinsic reactivity of the GP chars, we assume this to be the case and use the same value of ψ for all the LH chars.

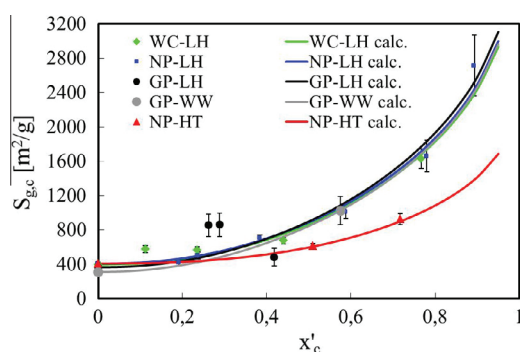


Fig. 4. Measured surface areas as a function of conversion for the chars of the cellulosic materials examined. The value of the structural parameter ψ for the different chars is listed in Table 5.

Table 5
The value of the structural parameter ψ for the different chars.

Char	ψ
WC-LH	6
NP-LH	6
NP-HT	1.8
GP-LH	8
GP-WW	10

Shown in Fig. 5 are normalized mass profiles for the char samples undergoing oxidation in 10 vol-% oxygen at 500 °C and 1 atm. The temperature profile used in the combustion tests is also shown. As can be observed, each sample dries completely and any carbon oxides on the carbonaceous material and the calcium carbonate decomposition products are completely removed at the end of the test during heating in nitrogen for 90 min.

At the 90 min mark when oxygen is admitted into the PTGA chamber, each char exhibits an initial rapid rate of mass loss. In the 10 vol-% O₂, 500 °C environment, the mass loss rate of the WC-LH char becomes essentially zero after about 200 min and the value of m/m_0 is near the ash content of the initial char (2.2% ash), indicating nearly complete burnout of the carbonaceous material in 200 min. The mass loss rate of the GP-LH char falls to a very low value in about 140 min, however the value of m/m_0 after 140 min of reaction time is greater than the ash content of the initial char (61.8% ash). This is another consequence of the large amount of CaCO₃ that was added during production of the paper in order to make it smooth and glossy. This CaCO₃ is converted to CaO at temperatures above 600–800 °C, which is the case in both the TF and LFR. This means that the fresh char inserted into the PTGA consist of small amounts of CaCO₃ but significant amounts of CaO, as can be seen from Tables 1 and 2. When CaO is exposed to CO₂ during the char oxidation process in the PTGA, a portion of the CO₂ is re-adsorbed to produce CaCO₃, which means that when all the carbon has been oxidized there are large amounts of CaCO₃ in the ash, making the ash significantly more massive than the ash containing just CaO. It can be shown from equilibrium calculations that the CO₂ is released when the temperature is increased beyond 600–800 °C.

After 330 min of reaction time in the reactive gas environment, the mass loss rates of the NP-LH and NP-HT chars are not yet zero and the values of m/m_0 are greater than the ash contents of the initial chars (11.5% and 17.7% ash, respectively for NP-LH and NP-HT), indicating that carbonaceous material remains in the PTGA balance pan. This is as expected since the reactivity and the conversion of the NP char has not yet reached zero. The NP-LH and NP-HT chars exhibit quite similar weight loss profiles, indicating little impact of ash content on the rate of mass loss. In addition, the similarity in mass loss rates indicates insignificant annealing of the carbonaceous material with heat treatment. This is characteristic of most biomass chars.

After 330 min of reaction time, nitrogen is readmitted into the PTGA reaction chamber, displacing the reactive gas, ending char oxidation. At 378 min, the temperature is ramped up to 1100 °C. During this heating period in nitrogen, surface oxide complexes are released as CO and CO₂ from the mass remaining in the PTGA

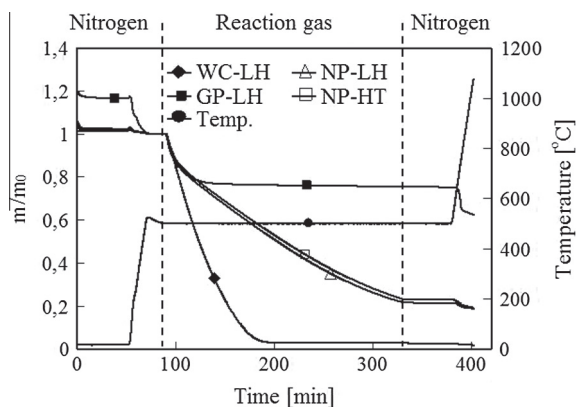


Fig. 5. Fractional mass remaining profiles for chars exposed to 10 vol-% oxygen at 500 °C.

balance pan: the mass of material in the balance pan decreases. In addition, for the GP the CaCO₃ is reduced to CaO while releasing CO₂. This results in a very strong mass loss for the GP as the temperature is increased above 600–800 °C, which is clearly seen in Fig. 5. The normalized mass at this time gives a true measure of the fraction of the initial mass of carbonaceous material remaining after oxidation for 330 min in the reactive gas environment. With the WC-LH char, less than 0.8% of the initial mass of carbonaceous material remained un-oxidized and with the NP-LH and NP-HT chars, from 10% to 5% of the initial mass of carbonaceous material remained unoxidized. Less than 2% of the initial mass of the carbonaceous portion of the GP-LH char remained un-oxidized under these oxidation conditions after 330 min. The thermograms shown in Fig. 5 are representative of duplicate oxidation tests and indicate that in the 10 vol-% O₂, 500 °C environment, the glossy paper char has the fastest initial mass loss rate and the newspaper chars have the slowest initial mass loss rates.

4.2. Char intrinsic chemical reactivity

In accord with Eq. (3), the mass loss data were combined with the mass specific surface area measurements to determine char reactivity for the chars examined. Each of the mass loss profiles (shown in Fig. 5, for example) was numerically differentiated to yield the conversion rate dx_c/dt as a function of conversion x_c , and combined with the least squares representation of the mass specific surface area (shown as the lines in Fig. 4)) to determine char reactivity as a function of conversion.

For the glossy paper, account was made for CO₂ uptake when calculating the reactivity. The sum of the mass of the carbonaceous part of the char, W_c , and the mass of the CO₂ capture by the calcium oxide, W_{CO_2} , is

$$W_{c,a} = W_c + W_{CO_2}. \quad (5)$$

The intrinsic reactivity of the carbonaceous part of the char is then given as

$$R_{ic} = \frac{1}{S_{gc}} \frac{1}{W_{c,a} - W_{CO_2,M}} \frac{dW_{c,a}}{dt} \quad (6)$$

where $W_{CO_2,M}$ is the mass of CO₂ capture by CaO in the char particle at full conversion. It can be assumed that the amount of CO₂ captured by the CaO in the ash scales linearly with conversion, such that

$$W_{CO_2} = W_{CO_2,M} x_c, \quad (7)$$

which is likely to be a good approximation since the amount of CaO exposed to the surroundings will scale almost linearly with conversion. Inserting $W_c = W_{c,0}(1 - x_c)$ and Eq. (7) into Eq. (5) yields the conversion for the GP char as

$$x_c = \frac{W_c + W_{CO_2} - W_{c,0}}{W_{CO_2,M} - W_{c,0}}. \quad (8)$$

The total mass of the char particle is given by $W_p = W_c + W_{CO_2} + W_{ash}$, when W_{ash} is the mass of the CO₂ free ash, such that the above equation can be re-written as

$$x_c = \frac{W_{p,0} - W_p}{W_{p,0} - W_{ash} - W_{CO_2,M}}. \quad (9)$$

The intrinsic reactivities of the chars of the materials selected for study as functions of conversion are shown in Fig. 6. All the chars have peak reactivity at low conversions ($x_c < 0.03$, daf). At extents of conversion greater than about 20% daf, the reactivities of the NP and GP chars have decreased by a factor ranging from 3 to 6 of the peak values. The glossy paper char has the highest peak reactivity and the newspaper chars, the lowest.

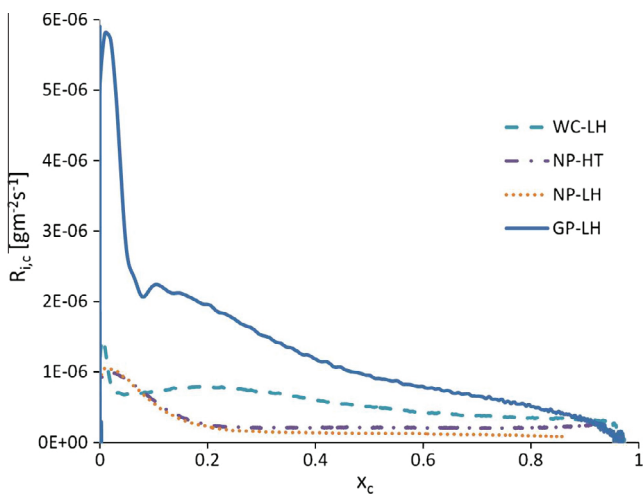


Fig. 6. Intrinsic reactivity (R_{ic}) as a function of conversion (x_c).

Table 6
Specific surface areas and peak and average reactivities.

Sample	S_{gp} (m ² /g)	$S_{gc,0}$ (m ² /g)	Peak R_{ic} (10 ⁻⁶ g/(s m ²))	\bar{R}_{ic} (10 ⁻⁶ g/(s m ²))
WC-LH	389 ± 12	398 ± 12	1.43 ± 0.04	0.46 ± 0.01
NP-LH	360 ± 14	407 ± 16	1.06 ± 0.04	0.21 ± 0.01
NP-HT	358 ± 11	409 ± 12	0.98 ± 0.03	0.27 ± 0.01
GP-LH	140 ± 41	366 ± 51	5.80 ± 0.40	1.36 ± 0.04

After the initial peak, the reactivity of the WC-LH char levels off at about 5% conversion. Thereafter, there is a slow increase in reactivity up to about 25% conversion before the reactivity starts to slowly decrease with increasing conversion. The reactivity of the WC-LH char levels off after about 70% conversion. Following the peak in the reactivity of the GP-LH char, the reactivity somewhat levels off at about 10% conversion before decreasing slowly until final burnout.

The NP-LH and NP-HT chars have similar reactivity profiles as a function of conversion. The reactivities of the newspaper chars level off after the peak at about 20% conversion, at which point the reactivity becomes relatively stable throughout the remainder of the oxidation process. The observed slight difference in the reactivity profiles of the NP-LH and NP-HT chars are likely to be a consequence of the uncertainty in the surface area measurements. The reactivity of NP-HT is seen to be similar to that of NP-LH throughout the lifetimes of the chars.

These experiments reveal that the reactivities of the cellulosic-based chars selected for study vary with conversion. One way of comparing the reactivity for the different chars is to compare the average reactivity over the whole conversion range. The average reactivity is calculated as follows:

$$\bar{R}_{ic} = \frac{\int_0^1 R_{ic}(x_c) dx_c}{\int_0^1 dx_c} \quad (10)$$

Table 7
Specific surface areas and reactivities for the glossy paper chars. The mass specific surface area of the carbonaceous part of GP-DS could not be determined because enough material was not available and the value has therefore been set equal to what was found for GP-LH.

Sample	Percentage ash	S_{gp} (m ² /g)	$S_{gc,0}$ (m ² /g)	Peak R_{ic} (10 ⁻⁶ g/(s m ²))	\bar{R}_{ic} (10 ⁻⁶ g/(s m ²))
GP-LH	61.8	140 ± 41	366 ± 51	5.80 ± 0.40	1.36 ± 0.04
GP-WW	53	147 ± 19	313 ± 41	2.80 ± 0.22	0.70 ± 0.02
GP-DS	37	140 ± 20	366 ± 51	1.20 ± 0.13	0.62 ± 0.05

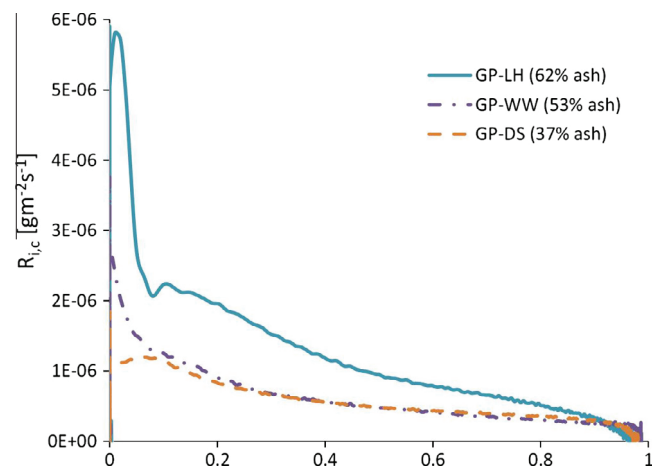


Fig. 7. Intrinsic reactivity as a function of conversion for the glossy paper chars.

Averaging R_{ic} over the entire conversion range removes the dependence of the reactivity on conversion and serves to rank the relative reactivities of the chars.

Presented in Table 6 are values determined for the peak and average intrinsic reactivities for each char, along with values for the initial specific surface areas. The average intrinsic reactivity of the NP-LH char ($0.21 \times 10^{-6} \text{ g m}^{-2} \text{ s}^{-1}$) is about 30% lower than that of the NP-HT char ($0.27 \times 10^{-6} \text{ g m}^{-2} \text{ s}^{-1}$), which is a factor of 1.6 lower than that of the WC-LH. The GP-LH char is about three times more reactive than the WC-LH char. Since the mass curves from the TGA results shown in Fig. 5 are rather similar it may be surprising that the mean reactivities of the two NP chars are relatively different (0.27 vs 0.21). The reason for this is that the NP-HT contains 50% more ash than the NP-LH char. The peak reactivities of the newspaper chars differ slightly, being $1.06 \times 10^{-6} \text{ g m}^{-2} \text{ s}^{-1}$ for NP-LH and $0.98 \times 10^{-6} \text{ g m}^{-2} \text{ s}^{-1}$ for NP-HT. The data for the NP-HT char do not indicate any large effect of heat treatment on the average intrinsic reactivity. The peak reactivity of the WC-LH char is only slightly more reactive than the NP chars, but it is less than a quarter as reactive as the GP-LH char (see Table 6).

4.3. Reactivity of glossy paper as a function of ash content

Shown in Fig. 7 are the intrinsic reactivities of the glossy paper char (GP-LH) and its ash-cleaned samples (GP-WW and GP-DS) as functions of conversion. The peak reactivities were lowered by reducing the ash contents of the chars. From 10% to full conversion, the intrinsic reactivities of the GP-WW and GP-DS chars are very similar, almost identical. Presented in Table 7 are the mass specific surface areas and peak and averaged reactivities for the glossy paper chars. The peak reactivity is lowered by as much as 70% when reducing the ash content from 62% to 37% by density separation of the char. The fraction of CO₂ released from CaCO₃ when heating the char to 1100 °C after oxidation has ended is equal to 13% for all the different GP chars. This indicates that the CaO is not washed away during the char washing process, the relative

content of the ash of the three different GP chars are therefore different.

5. Conclusions

The intrinsic reactivity of three different chars formed under low heating rate conditions from cellulosic wastes have been investigated. The average intrinsic reactivities for the three chars, during reaction in 10 vol.% oxygen at 500 °C and atmospheric pressure, were found to be 0.46×10^{-6} , 0.21×10^{-6} and $1.36 \times 10^{-6} \text{ g m}^{-2} \text{ s}^{-1}$, respectively, for the WC-LH, NP-LH and GP-LH chars and the corresponding peak reactivities were 1.43×10^{-6} , 1.06×10^{-6} and $5.80 \times 10^{-6} \text{ g m}^{-2} \text{ s}^{-1}$. The reactivities for WC-LH, NP-LH and GP-LH differ as a function of conversion and ash content. However, for these cellulosic-based chars no trend in terms of either increasing or decreasing reactivity with increasing ash content was found. Moderate heat treatment had no significant influence on char reactivity. A heat-treated sample of the newspaper char (NP-HT) behaved essentially the same as its parent char (NP-LH).

Due to the CaCO_3 that is used in the production of glossy paper, it is crucial to account for the release and capture of CO_2 onto the CaCO_3/CaO in the ash. Unless accounted for, this will artificially make the reactivity measured in a TGA too low and the remaining ash content too high.

Reducing the ash content of the GP-LH char from 62% to 37% resulted in a char with a lower peak reactivity at low conversion. At conversions less than 5%, reducing the ash content clearly lowers the reactivity. This suggests, perhaps, a catalytic influence of the ash. It is likely that the ash also plays a role in limiting the reactivity by for example, encapsulating the carbonaceous material, making it more difficult for oxygen to reach the carbonaceous surfaces where it can be adsorbed.

Acknowledgments

SINTEF Energy Research (Norway), The Norwegian Research Council supporting the “Environmental and Process Control

project” at SINTEF Materials Technology (Norway) and the Global Climate Energy Project (GCEP) at Stanford University (US) are acknowledged for the financial support of this work. Ph.D. student Liqiang Ma (Stanford University) is acknowledged for helping out with the LFR tests. NELH also acknowledges the CAMPS project supported by the Research Council of Norway (215707). The work has additionally been produced with support from the BIGCCS Centre, performed under the Norwegian research program Centres for Environment-friendly Energy Research (FME). The authors acknowledge the following BIGCCS partners for their contributions: Aker Solutions, ConocoPhillips, Gassco, Shell, Statoil, TOTAL, GDF SUEZ and the Research Council of Norway (193816/S60).

References

- [1] Grønli MG. A theoretical and experimental study of the thermal degradation of biomass. PhD thesis. The Norwegian University of Science and Technology; 1996.
- [2] Sørum L, Grønli MG, Hustad JE. Pyrolysis characteristics and kinetics of municipal solid wastes. *Fuel* 2001;80:1217–27.
- [3] Sørum L, Glarborg P, Jensen A, Skreiberg Ø, Dam-Johansen K. Formation of NO from combustion of volatiles from municipal solid wastes. *Combust Flame* 2001;124:195–212.
- [4] Mitchell RE, Hurt RH, Baxter LL, Hardesty DR. Compilation of Sandia coal char combustion data and kinetic analyses: milestone report. Sandia National Laboratories, SAND92-8208; 1992.
- [5] Miles TA, Miles Jr TA, Baxter L, Brywers RW, Jenkins BM, Oden LL. Alkali deposits found in biomass power plants a preliminary investigation of their extent and nature. National Energy Laboratory, NREL/TP-433-8142; 1995.
- [6] Tsai NK-C. Influences of high carbon monoxide concentration on the carbon dioxide gasification of a selected coal char. PhD thesis. Mechanical Engineering Dept., Stanford University; 1999.
- [7] Brunauer S, Emmett PH, Teller EJ. Adsorption of gases in multimolecular layers. *Am Chem Soc* 1938;60:309–19.
- [8] Mahajan OP, Walker Jr PL. Porosity of coals and coal products. In: Karr C, editor. *Analytical methods for coal and coal products*, vol. 1. New York: Academic Press; 1978. p. 125.
- [9] Walker Jr PL, Patel RL. Surface areas of coals from carbon dioxide adsorption at 298 °K. *Fuel* 1970;49:91–4.
- [10] Campbell PA, Mitchell RE, Ma L. Characterization of coal char and biomass char reactivities to oxygen. *Proc Combust Inst* 2002;29:519–26.
- [11] Bhatia SK, Perlmutter DD. A random pore model for fluid-solid reactions: I. Isothermal, kinetic control. *AIChE J* 1980;26:379–86.